

BIMA CO OBSERVATION OF EP AQUARI: THE SEMIREGULAR PULSATING STAR WITH A DOUBLE-COMPONENT LINE PROFILE

JUN-ICHI NAKASHIMA¹

Department of Astronomy, University of Illinois at Urbana-Champaign, 1002 West Green Street, Urbana, IL 61801; junichi@asiaa.sinica.edu.tw
Received 2005 July 26; accepted 2005 October 18

ABSTRACT

This paper reports the results of a Berkeley-Illinois-Maryland Association array interferometric observation of EP Aqr, a semiregular pulsating star with a double-component line profile in the CO $J = 1-0$ line. The broad component shows a flat-topped profile, and the narrow component shows a spiky strong peak. Although previous single-dish observations suggested that the CO $J = 2-1$ line exhibits a Gaussian-like profile, the CO $J = 1-0$ line does not. The spatial distributions of both the narrow and the broad components appear to be roughly round with the same peak positions. No significant velocity gradient is seen. The spatial-kinetic properties of the molecular envelope of EP Aqr are reminiscent of a multiple-shell structure model rather than of a bipolar flow and disk model. A problem with this interpretation is that no evidence of interaction between the narrow- and broad-component regions is seen. A Gaussian-like feature seen in the CO $J = 2-1$ line might play a key role in understanding the spatiokinetic properties of the molecular envelope of EP Aqr.

Subject headings: circumstellar matter — stars: AGB and post-AGB — stars: imaging — stars: individual (EP Aquarii) — stars: late-type — stars: mass loss

1. INTRODUCTION

Asymptotic giant branch (AGB) stars occasionally exhibit a molecular line profile with very small line widths less than 5 km s^{-1} , much smaller than typical AGB outflow velocities. Such a narrow line profile is usually superimposed on a broad pedestal component (this profile is often called a “double-component profile” or a “composite profile”) but is sometimes independently found without the broad component (Knapp et al. 1998; Kerschbaum & Olofsson 1999; Winters et al. 2003). A non-negligible number of AGB stars exhibit a narrow line; in fact, the narrow line has been detected in 5%–10% of a sample of AGB stars (Winters et al. 2003). Narrow line profiles have been detected toward a wide variety of AGB stars. For instance, Knapp et al. (1998) reported narrow lines detected toward both M- and C-type AGB stars; several semiregular pulsating stars also exhibit narrow lines (Kerschbaum & Olofsson 1999).

AGB stars exhibiting a narrow line profile are notable in some respects. First, chemically unusual AGB stars occasionally exhibit a narrow line profile. For instance, Kahane & Jura (1996) reported double-component profiles in the CO radio lines of BM Gem and EU And; these stars are “silicate carbon stars,” which simultaneously have a carbon-rich (C-rich) central star and oxygen-rich (O-rich) circumstellar material. Nakashima et al. (2004) have found a double-component profile in radio molecular spectra of IRAS 19312+1950, an SiO maser source with a rich set of molecular species, and have suggested that this object is identified as an O-rich AGB (or post-AGB) star (Nakashima & Deguchi 2000, 2004, 2005; Nakashima et al. 2004). Second, according to recent observations, some AGB stars exhibiting a narrow line profile might harbor a Keplerian rotation disk. Bergman et al. (2000) have reported a tentative detection of such a disk in RV Boo, an O-rich AGB star with a double-component profile. Similarly, the existence of a Keplerian rotation disk has been observationally suggested in X Her, which is also an O-rich AGB

star with a double-component profile (Nakashima 2005). Although a physical relationship between narrow lines, chemical peculiarity, and a Keplerian rotation disk is still unclear, Kahane & Jura (1996) have suggested that narrow lines found in silicate carbon stars might be explained by gravitationally stable material in the form of a distorted or puffed-up slowly rotating disk, in which O-rich material is trapped. In contrast, to explain a double-component profile, Knapp et al. (1998) have advanced a hypothesis that takes a multiple-shell structure into account, in which each shell has different expanding velocities produced by episodic mass loss with highly varying gas expansion velocities.

EP Aqr is a semiregular variable (SRb) with a period of ~ 55 days (this period is uncertain) at a distance of 135 pc; its spectral type is M8 III (Perryman et al. 1997). Dumm & Schild (1998) evaluated the stellar effective temperature at 3236 K. Winters et al. (2003) and Knapp et al. (1998) have produced high-velocity-resolution spectra of the CO $J = 1-0$, $2-1$, and $3-2$ lines. All three lines show a double-component profile with a narrow component ($V_{\text{exp}} \sim 1.4 \text{ km s}^{-1}$) superimposed on a broad pedestal component ($V_{\text{exp}} \sim 11 \text{ km s}^{-1}$), both centered at $V_{\text{lsr}} \sim -34 \text{ km s}^{-1}$. The mass-loss rates derived from these CO observations are $2.3 \times 10^{-7} M_{\odot}$ (broad component) and $1.7 \times 10^{-8} M_{\odot}$ (narrow component). Kerschbaum & Olofsson (1999) have reported the same value for the center velocity ($\sim -33.7 \text{ km s}^{-1}$) of the two CO $J = 1-0$ components. However, Olofsson et al. (2002) obtained slightly lower expansion velocities, 1.0 and 9.0 km s^{-1} , through a line-fit accounting for turbulence. EP Aqr has also been detected in the SiO ($v = 0$, $J = 2-1$ and $3-2$) thermal emission by González Delgado et al. (2003). Both lines are centered at $V_{\text{lsr}} \sim -32 \text{ km s}^{-1}$ and have a width corresponding to $V_{\text{exp}} \sim 8 \text{ km s}^{-1}$. Both lines have spectral profiles with only one component.

This paper reports the results of a high-angular-resolution CO observation of EP Aqr with the Berkeley-Illinois-Maryland Association (BIMA) array. The main objectives of this research are (1) to investigate spatiokinematic properties of the circumstellar molecular envelope of EP Aqr with a high-angular-resolution observation and (2) to compare the spatiokinetic properties with

¹ Current address: Institute of Astronomy and Astrophysics, Academia Sinica, P.O. Box 23-141, Taipei 106, Taiwan.

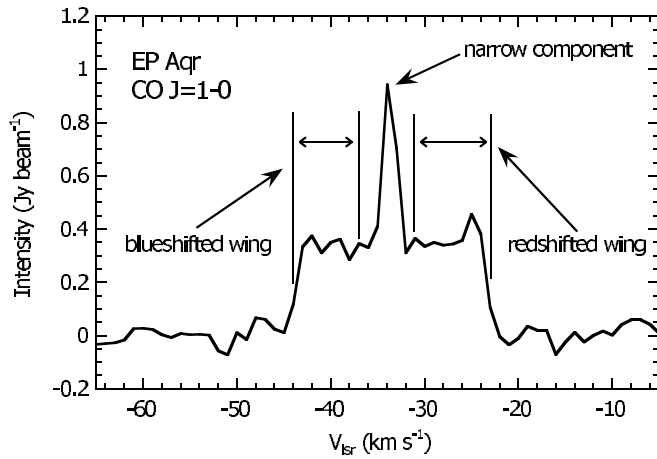


FIG. 1.—Spatially averaged spectrum of EP Aqr in the CO $J=1-0$ line. The averaged area is a circle with a diameter of $15''$; the averaging circle is centered on the mapping center. The vertical solid lines represent the velocity ranges selected for the blue- and redshifted halves of the broad component. Each component is indicated.

those of other AGB stars with a double-component profile (e.g., X Her and RV Boo). As a result, the spatiokinetic properties of EP Aqr are found to be very different from those of X Her and RV Boo.

2. OBSERVATION AND RESULTS

Interferometric observations of the CO $J=1-0$ line at 115.271202 GHz in EP Aqr were made with the BIMA array from 2004 January to March. The instrument was described in detail by Welch et al. (1996). The array used 10 elements in three configurations (B, C, and D). The observations were interleaved every 25 minutes with the nearby point sources P2134+00 and 2148+069 to track the phase variations over time. The absolute flux calibration was determined from observations of Uranus and MWC 349 and is accurate to within 20%. The final map has an

accumulated on-source observing time of about 12.3 hr. Typical single-sideband system temperatures range from 250 to 500 K. The velocity coverage is about 350 km s^{-1} , using three different correlator windows with a bandwidth of 50 MHz each. The velocity resolution is 1.03 km s^{-1} . The phase center of the map is R.A. = $21^{\text{h}}46^{\text{m}}31^{\text{s}}.849$, decl. = $-2^{\circ}12'45''.923$ (J2000.0). Data reduction was performed with the MIRIAD software package (Sault et al. 1995). Standard data reduction, calibration, imaging, and deconvolution procedures were followed. Robust weighting of the visibility data gives a $5''.15 \times 3''.68$ CLEAN beam with a position angle of $10^{\circ}.4$. The rms noise per 1.0 km s^{-1} is $1.5 \times 10^{-1} \text{ Jy beam}^{-1}$.

Figure 1 shows a spatially averaged spectrum of EP Aqr in the CO $J=1-0$ line. The averaged area is a circle with a diameter of $15''$ centered at the phase center. A double-component profile is clearly seen in the spectrum as reported in previous papers (Knapp et al. 1998; Winters et al. 2003). The broad pedestal component shows a flat-topped profile, and the narrow component shows a strong spiky peak. Winters et al. (2003) pointed out that the line profile of the narrow component in the $^{12}\text{CO } J=2-1$ line appears to be Gaussian; however, we do not have the spatial resolution to confirm this. The narrow component peaks at $V_{\text{lsr}} = -34 \text{ km s}^{-1}$, and its expansion velocity is calculated to be 2.1 km s^{-1} by fitting a parabola. The expansion velocity of the broad component is 10 km s^{-1} ; this is a half-maximum width of the line at the zero intensity. The central velocity of the broad component is -34 km s^{-1} . These line parameters are consistent with previous values. In comparison with the single-dish spectrum taken by the 15 m Swedish-ESO Submillimetre Telescope (SEST; Kerschbaum & Olofsson 1999), roughly 90% of the single-dish flux is recovered in the present interferometric observation. To check the continuum emission, frequency channels were integrated over 150 MHz using the sideband opposite the line observation. The upper limit of the continuum flux at the 3 mm band (center frequency $\sim 112 \text{ GHz}$) is $1.9 \times 10^{-2} \text{ Jy}$.

The left panel of Figure 2 shows velocity-integrated intensity maps in the CO $J=1-0$ line; for comparison, the right panel

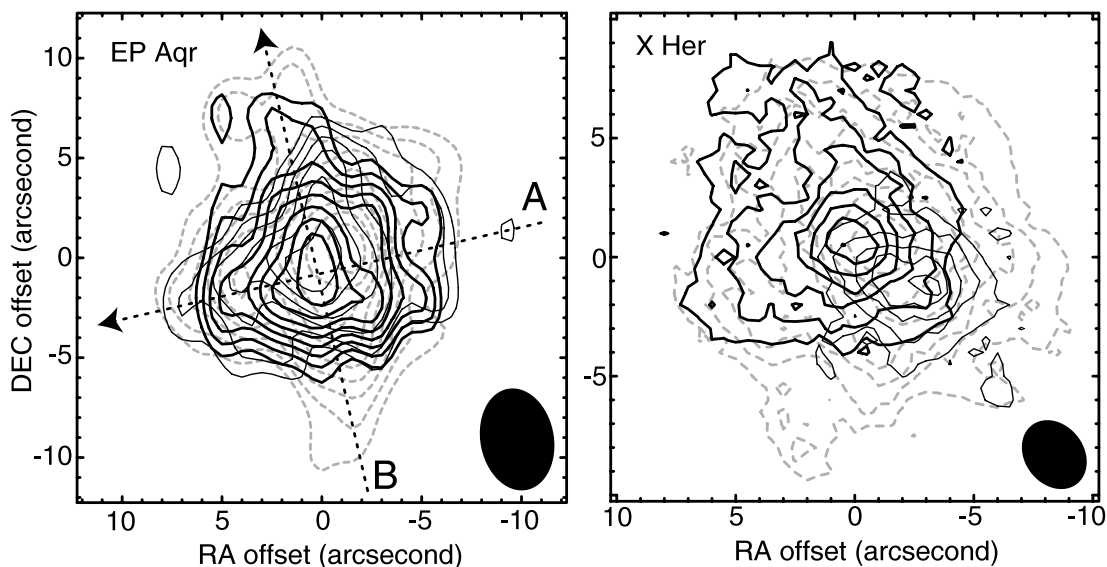


FIG. 2.—*Left*: Velocity-integrated intensity maps of EP Aqr. The thick and thin contours map the blue- and redshifted wings of the broad component, respectively; the gray dashed contours map the narrow component. The synthesized beam size is indicated in the bottom right corner. The contours start at the 5σ level, with increments every 2σ . The 1σ levels for the thick, thin, and dashed contours are 5.1×10^{-2} , 5.1×10^{-2} , and $8.9 \times 10^{-2} \text{ Jy beam}^{-1}$. The velocity integration ranges for the blue- and redshifted wings are -44 to -37 and -31 to -23 , respectively; the width of the integration range of the narrow component is 3 km s^{-1} (the peak velocity is taken at the center of the range). The dotted arrows represent the cuts used for Fig. 3. *Right*: Similar map of X Her (taken from Nakashima 2005), for comparison. The contours are the same as in the left panel (see Nakashima 2005 for details).

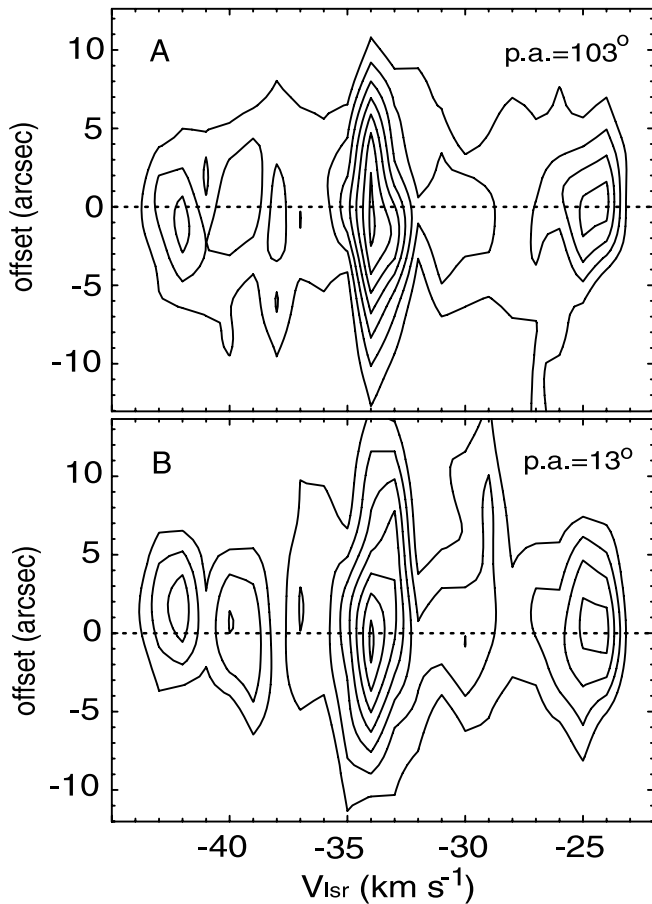


FIG. 3.—Position-velocity diagrams for the cuts indicated in Fig. 2. The contours start at the 2σ level, with increments every 1σ . The 1σ level is 1.5×10^{-1} Jy beam $^{-1}$. The names of the cuts and the position angles are indicated in the top left and top right corners of each panel, respectively. The dashed horizontal lines represent the origin of the offset axes.

shows similar maps of X Her in the CO $J = 1-0$ line, which also has a double-component line profile. (The X Her maps are taken from Nakashima [2005]; the recovered rate of the Institut de Radioastronomie Millimétrique [IRAM] single-dish flux has been confirmed to be more than 95%—this was incorrectly given as 5% by Nakashima [2005].) The thick and thin contours represent the blue- and redshifted wings of the broad component, respectively; the lowest contours correspond to a 5σ level, which was measured in an emission-free region in the images. The dashed gray contours represent the narrow component. Usage of contours is common in the right and left panels. At a glance, the overall structure of the molecular envelope of EP Aqr, which is clearly resolved by our synthesized beam, is significantly different from that of X Her. As reported by Nakashima (2005), X Her exhibits a bipolar flow (corresponding to the thick and thin contours) and a possible disk (corresponding to the dashed contours). In contrast, all the thick, thin, and dashed contours in the left panel appear to be roughly round, and the positions of the intensity peaks of the three components correspond within a beam size. Interestingly, the three components exhibit almost the same spatial sizes, although the narrow component is slightly elongated in the north-south direction. The diameter of the round structure seen in the left panel of Figure 2 is about $15''$, corresponding to 3.0×10^{16} cm at a distance of 135 pc. For better understanding of the spatiokinetic properties, a position-velocity diagram is presented in Figure 3. Because the narrow-

component region is slightly extended in the north-south direction, one of the cuts used for Figure 3 (cut A) is taken along the north-south elongation of the narrow-component region, and another cut (cut B) is taken in the perpendicular direction. No significant velocity gradients are seen at these or other position angles. In Figure 3, the spatial size of the broad-component region (represented in the vertical axes) is apparently smaller than that of the narrow component; however, this is due to a low signal-to-noise ratio in the corresponding velocity range. In fact, the size of the broad-component region seen in the velocity-integrated intensity map (see Fig. 2) is almost the same as that of the narrow-component region.

3. DISCUSSION

Until now, two AGB stars with a double-component profile have been observed with radio interferometers in the CO $J = 1-0$ line (i.e., RV Boo and X Her; Bergman et al. 2000; Nakashima 2005). These are all O-rich semiregular pulsating stars. However, the spatiokinetic properties of EP Aqr are clearly different from those of X Her and RV Boo, as seen in § 2. If this is real, AGB envelopes with a double-component line profile include at least two types of kinematics. As stated in § 1, two hypotheses have been proposed to explain a double-component profile: a slowly rotating puffed-up disk with a bipolar flow (Kahane & Jura 1996) and a double-shell structure, in which each shell has different expanding velocities produced by episodic mass loss with highly varying gas expansion velocities (Knapp et al. 1998). Previous observations suggested that the spatiokinetic properties of X Her and RV Boo could possibly be explained by the disk and bipolar flow model. In contrast, the properties of EP Aqr are rather reminiscent of the multiple-shell model because no significant velocity gradient is seen in the position-velocity diagrams and because the overall structure of the CO emission region is roughly round rather than bipolar. One might consider the possibility that the properties of EP Aqr are explained by a disk and bipolar flow model if we assume a pole-on view; however, such a case is unlikely.

A problem with the interpretation as a multiple (double) shell structure is that we cannot see any evidence of physical interaction between the narrow- and broad-component regions in the present observation. According to the spatial sizes and expanding velocities, the dynamical timescales of the narrow- and broad-component regions are roughly estimated to be 1270 and 160 yr, respectively; these timescales are similar to that of a typical AGB circumstellar envelope. The similar spatial scales but different timescales show that physical interaction must take place, but we see no observational evidence for this. For example, if material of the narrow-component region is swept up by that of the broad component, the swept up material should be seen as a ringlike feature in the left panel of Figure 2. As pointed out in § 2, the narrow component of the CO $J = 2-1$ line detected in the previous single-dish observation exhibits a Gaussian profile; in contrast, the CO $J = 1-0$ line does not show such a Gaussian profile. This difference might potentially mean that an interacting region between the narrow- and broad-component regions cannot be easily detected in the CO $J = 1-0$ line: if the interacting region has a high temperature, it might not be easily seen in the CO $J = 1-0$ line. Furthermore, if the interacting region has a high turbulence velocity caused by the interaction, the Gaussian profile seen in the CO $J = 2-1$ line might be produced by the turbulence. (Of course, the absence of the Gaussian wing in the CO $J = 1-0$ line might be just a signal-to-noise ratio issue.) To check this conjecture, CO mapping observations in the CO $J = 2-1$ line are required.

4. SUMMARY

This paper has reported the results of BIMA observations of a semiregular pulsating star with a double-component line profile, EP Aqr, in the CO $J = 1-0$ line. The main results are as follows:

1. A double-component profile is clearly seen in the spectrum as reported in the previous observations. The broad component shows a flat-topped profile, and the narrow component is a spiky strong peak. A Gaussian profile, which has been seen in the $J = 2-1$ line, is not confirmed in the CO $J = 1-0$ line.

2. Intensity maps of both the narrow and broad components are roughly round and centered at the same position. No significant velocity gradient is seen in the position-velocity diagrams.

3. The spatial-kinetic properties of EP Aqr are rather reminiscent of the multiple-shell model suggested by Knapp et al.

(1998). A problem with this interpretation is that no evidence of physical interaction between the narrow- and broad-component regions is seen in the present observation. A Gaussian-like wing feature seen only in the CO $J = 2-1$ line might play a key role in understanding this problem.

The author thanks Shuji Deguchi for useful discussions. The author also thanks Jill Knapp, whose comments and suggestions as a referee were very helpful in improving the manuscript. This research has been supported by the Laboratory for Astronomical Imaging at the University of Illinois and by NSF grant AST 02-28953 and has made use of the SIMBAD and ADS databases.

REFERENCES

- Bergman, P., Kerschbaum, F., & Olofsson, H. 2000, *A&A*, 353, 257
 Dumm, T., & Schild, H. 1998, *NewA*, 3, 137
 González Delgado, D., Olofsson, H., Kerschbaum, F., Schöier, F. L., Lindqvist, M., & Groenewegen, M. A. T. 2003, *A&A*, 411, 123
 Kahane, C., & Jura, M. 1996, *A&A*, 310, 952
 Kerschbaum, F., & Olofsson, H. 1999, *A&AS*, 138, 299
 Knapp, G. R., Young, K., Lee, E., & Jorissen, A. 1998, *ApJS*, 117, 209
 Nakashima, J. 2005, *ApJ*, 620, 943
 Nakashima, J., & Deguchi, S. 2000, *PASJ*, 52, L43
 ———. 2004, *ApJ*, 610, L41
 ———. 2005, *ApJ*, 633, 282
 Nakashima, J., Deguchi, S., & Kuno, N. 2004, *PASJ*, 56, 193
 Olofsson, H., González Delgado, D., Kerschbaum, F., & Schöier, F. L. 2002, *A&A*, 391, 1053
 Perryman, M., et al. 1997, *A&A*, 323, L49
 Sault, R. J., Teuben, P. J., & Wright, M. C. H. 1995, in *ASP Conf. Ser. 77, Astronomical Data Analysis Software and Systems IV*, ed. R. A. Shaw, H. E. Payne, & J. J. E. Hayes (San Francisco: ASP), 433
 Welch, W. J., et al. 1996, *PASP*, 108, 93
 Winters, J. M., Le Bertre, T., Jeong, K. S., Nyman, L.-Å., & Epchtein, N. 2003, *A&A*, 409, 715